Differential regulation and synthetic lethality of exclusive *RB1* and *CDKN2A* mutations in lung cancer

NAYOUNG KIM[1,3], MEE SONG[1], SOMIN KIM[1], YUJEONG SEO[3], YONGHWAN KIM[3] and SUKJOON YOON[1,2]

[1]Center for Advanced Bioinformatics and Systems Medicine, [2]Department of Biological Sciences, Sookmyung Women's University; [3]Department of Life Systems, Sookmyung Women's University, Seoul, Republic of Korea

Received October 1, 2015; Accepted October 26, 2015

DOI: 10.3892/ijo.2015.3262

Abstract. Genetic alterations in lung cancer are distinctly represented in non-small cell lung carcinoma (NSCLC) and small cell lung carcinoma (SCLC). Mutation of the *RB1* and *CDKN2A* genes, which are tightly associated with cell cycle regulation, is exclusive to SCLC and NSCLC cells, respectively. Through the systematic analysis of transcriptome and proteome datasets for 318 cancer cell lines, we characterized differential gene expression and protein regulation in *RB1*-mutant SCLC and *CDKN2A*-mutant NSCLC. Many of the genes and proteins associated with *RB1*-mutant SCLC cell lines belong to functional categories of gene expression and transcription, whereas those associated with *CDKN2A*-mutant NSCLC cell lines were enriched in gene sets of the extracellular matrix and focal adhesion. These results indicate that the loss of RB1 and CDKN2A function induces distinctively different signaling cascades in SCLC and NSCLC cells. In addition, knockdown of the *RB1* gene in *CKDN2A*-mutant cell lines (and vice versa) synergistically inhibits cancer cell proliferation. The present study on the exclusive role of *RB1* and *CDKN2A* mutations in lung cancer subtypes demonstrates a synthetic lethal strategy for cancer regulation.

Introduction

Understanding heterogeneous genetic alterations in tumors is recognized as a key factor in advancing cancer therapy (1-3). Lung cancers are classified into two subtypes, non-small cell lung carcinoma (NSCLC) and small cell lung carcinoma (SCLC), which harbor exclusive specific mutations: *RB1* in SCLC and *CDKN2A* ($p16^{INK4A}$) in NSCLC (4). Both the *RB1* and *CDKN2A* genes are tightly associated with cell cycle regulation, and *CDKN2A* regulates RB1 phosphorylation through cyclin E and D1 (5,6). The crucial role of RB1 as a regulator in cell cycle progression has been intensively investigated (7-9). Accumulated data have demonstrated mutually exclusive mutation patterns for genes encoding proteins that function in the same biological pathway. For instance, mutations of the *KRAS* or *BRAF* gene, which are downstream of the EGFR signaling pathway, have not been found in *EGFR*-mutated NSCLC (10,11), and co-mutations of the *TP53* and *PIK3CA* pair (12) or the *RB1* and *CDKN2A* pair (13) rarely occur in the same tumors. However, the biological meaning of such mutually exclusive mutation patterns is not fully understood, even though this exclusiveness does serve as an attractive target for the development of novel therapeutics (14).

An understanding of differential regulation along with distinct mutations in *RB1* and *CDKN2A* is required to identify molecular characteristics of the progression of SCLC and NSCLC subtypes. Large-scale cell line-based high-throughput transcriptome and proteome datasets facilitate the understanding of molecular characterization of cancers through genome-wide functional analyses. The National Cancer Institute (NCI) released well-annotated sets of both DNA microarray data to detect the gene expression and reverse-phase protein array (RPPA) data to detect the total protein and phosphorylation on 60 well-characterized cancer cell lines (15). Diverse omics datasets on an expanded panel of >300 cancer cell lines were also generated by GlaxoSmithKline (GSK) (16). Together with these datasets, the extensive mutation profile on individual cell lines is available from the COSMIC (Catalogue of Somatic Mutations in Cancer) database (17). Through mutation-oriented association studies on cell line-based omics data, we have reported new targets and mechanisms for cancer regulation (3,18,19).

In the present study, the regulation of gene and protein levels driven by *RB1* or *CDKN2A* mutations in lung cancer was analyzed using transcriptome and proteome datasets obtained from 318 diverse cancer cell lines. We attempted to identify the differentially regulated gene/protein signatures and functional pathways specific to *RB1* and *CDKN2A* mutations. Furthermore, we experimentally investigated whether double or complementary knockdown of *RB1* or *CDKN2A* gene expression has a specific effect on the reciprocal mutant subtype in lung cancer cell lines. We expect that this study will provide a useful resource for the regulation of lung cancer

Correspondence to: Professor Sukjoon Yoon, Center for Advanced Bioinformatics and Systems Medicine, Department of Biological Sciences, Sookmyung Women's University, Hyochangwon-gil 52, Yongsan-gu, Seoul 140-742, Republic of Korea
E-mail: yoonsj@sookmyung.ac.kr

Key words: cancer cell line panel, *RB1*, *CDKN2A*, gene expression, reverse-phase protein array, lung cancer

progression using synergistic mechanisms of exclusive *RB1* or *CDKN2A* mutations.

Materials and methods

Data acquisition. The large-scale transcriptome dataset on 318 cancer cell lines was obtained from the Cancer Biomedical Informatics Grid (caBIG) website (https://cabig.nci.nih.gov/caArray_GSKdata) (16). This dataset, also known as the GlaxoSmithKline (GSK) dataset, has 950 arrays performed in triplicate for each cell line with the Affymetrix U133 Plus 2.0 Array chip. It was normalized to MAS5 and then transformed to a log2 scale.

The reverse-phase protein array (RPPA) dataset to detect protein expression and phosphorylation was generated in the Functional Proteomics Core of the M.D. Anderson Cancer Center using a total of 179 cancer cell lines, which were included in the transcriptome dataset. These cell lines were purchased from several vendors (American Type Culture Collection; Developmental Therapeutics Program, National Cancer Institute; German Resource Centre for Biological Material and European Collection of Animal Cell Cultures) and grown in standard culture media as recommended by the vendor. The genetic identity of cell lines was determined by cross comparing all cell lines in this set (16,20). The cells were maintained in RPMI-1640 supplemented with 5% fetal bovine serum at 37˚C in a humidified 5% CO_2 atmosphere. Proteins were harvested when the cells reached ~70% confluence. The cells were lysed in buffer containing 1% Triton X-100, 50 mM HEPES pH 7.4, 150 mM NaCl, 1.5 mM $MgCl_2$, 1 mM ethylene glycol tetraacetic acid, 100 mM NaF, 10 mM NaPPi, 10% glycerol, 1 mM Na_3VO_4 and complete protease inhibitor cocktail (Roche Diagnostics). Protein supernatants were isolated using standard methods (21), and the protein concentration was determined using the bicinchoninic acid assay (22). Samples were diluted to a uniform protein concentration and denatured in 1% sodium dodecyl sulfate for 10 min at 95˚C. Samples were stored at -80˚C until use. RPPA analysis was performed as described previously (21,23,24). A logarithmic value reflecting the relative amount of each protein in each sample was generated for subsequent analyses. The RPPA analysis was performed using a total of 115 antibodies.

The annotation of somatic mutation on all cell lines was organized by the COSMIIC (Catalogue of Somatic Mutations in Cancer) database (http://cancer.sanger.ac.uk/cosmic) (17).

Enrichment analysis of somatic mutations. To describe the selectivity of mutation occurrence, we calculated enrichment scores using an odds ratio between the observed odds and expected odds. The observed odds score is the ratio for the number of mutated cell lines in a specific cancer type via the number of cell lines in a specific cancer type. The expected odds score is the ratio for the number of mutated cell lines vs. the total number of cell lines. In addition, the probability of an odds ratio was calculated by the Fisher exact test using the R open-source computing language, version 2.15. The Fisher exact test uses a hypergeometric distribution to determine the significance of the agreement between individual question pairs (25).

Mutation-specific gene and protein expression analysis. For the selection of *RB1* and *CDKN2A* mutation-specific gene and protein expression markers together with excluding the subtype-dependent expressions, lung cancer cell lines were classified into two groups: NSCLC and SCLC. Then, we divided the cell lines of each subtype into two groups based on the mutational status of *RB1* and *CDKN2A*. *CDKN2A*-mutant and wild-type cell lines were mainly considered in the NSCLC type. *RB1*-mutant and wild-type cell lines were considered in the SCLC type. As a result, in the transcriptome dataset, we classified 9, 16, 22 and 24 cell line samples into the following four groups, respectively: RB1*wt* SCLC; RB1*mt* SCLC; CDKN2A*wt* NSCLC; and CDKN2A*mt* NSCLC. In the RPPA dataset, we classified 4, 7, 4 and 16 cell line samples into four groups, respectively: RB1*wt* SCLC; RB1*mt* SCLC; CDKN2A*wt* NSCLC; and CDKN2A*mt* NSCLC. The gene expression was detected using a $\log_2$ fold change value for the average difference of mutant and wild-type cell lines. The significance was confirmed by a t-test.

The patterns of gene expression were analyzed through a hierarchical clustering method. The clustering and its visualization on a heatmap were performed using the software QCanvas (26). QCanvas can be downloaded freely from the website http://compbio.sookmyung.ac.kr/~qcanvas.

Gene set enrichment analysis. Pathway analysis was performed using the GSEA (Gene Set Enrichment Analysis) method (27). Gene sets, integrated from Reactome, PID, KEGG, and Biocarta database, were obtained from the online pathway database, MSigDB v3.1 (http://www.broadinstitute.org/gsea/msigdb). The significantly ($p<0.01$) enriched gene sets among the results of the GSEA were reorganized based on major functional categories in each database.

Cell culture. NCI-60 lung cancer cell lines (NCI-H460, A549, NCI-H322M, NCI-H226, EKVX, and NCI-H23) were obtained from National Cancer Institute (NCI DTP), USA. NCI-H1993, NCI-H1935, NCI-H82 and NCI-H524 were obtained from American Type Culture Collection (ATCC). All cells were grown in RPMI-1640 medium (HyClone, USA) with 10% FBS (HyClone) and 1% penicillin/streptomycin (Gibco, USA), and maintained at 37˚C in a humidified atmosphere at 5% CO_2.

siRNA transfection and cell viability assay. To detect cell viability after siRNA transfection, the cells were seeded in a 96-well plate at a density of 5,000 cells per well. After adhering for 24 h, target siRNAs were added in transfection medium (Gibco) for 6 h at 37˚C in a CO_2 incubator. siRB1 (L-003296-02), siCDKN2A (L-011007-00) and non-targeting siRNA (D-001810-10) were purchased from Dharmacon Inc. (Lafayette, CO, USA). After being cultured for 72 h at 37˚C, 5% CO_2, cell viability was detected using a CellTiter-Blue Cell Viability Assay (Promega, Madison, WI, USA).

Results and Discussion

RB1 and CDKN2A mutations in SCLC and NSCLC cell lines. Genetic alterations affecting the same biological pathway are generally not found in the same cancer cell. Accordingly, exclusive mutation patterns of *RB1* and *CDKN2A* genes

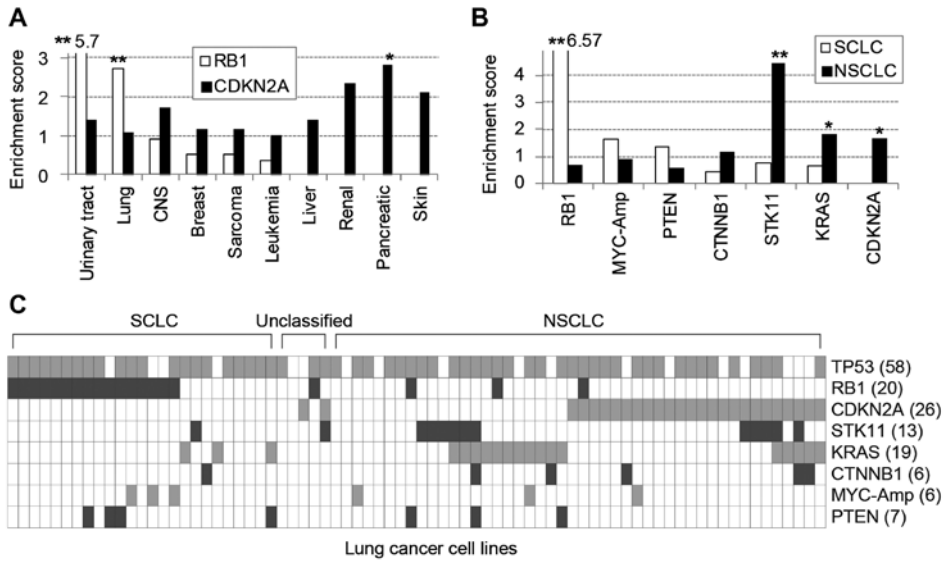

Figure 1. *RB1* and *CDKN2A* mutation frequency in the cancer cell line panel. (A) Enrichment score of *RB1* and *CDKN2A* mutation frequency among diverse cancer lineages. The enrichment score was calculated by the odds ratio between the observed and expected odds. The observed odds ratio is the ratio for *RB1* or *CDKN2A* mutation among each cancer type. The expected odds ratio is the ratio for *RB1* or *CDKN2A* mutation among all 318 cell lines. (B) The enrichment score of major mutation frequency in non-small cell lung cancer (NSCLC) and small cell lung cancer (SCLC). The observed odds ratio is the ratio for each mutation frequency in 46 NSCLC or 25 SCLC cell lines. The expected odds ratio is the ratio for each mutation frequency in all 318 cell lines. (C) The distribution of major gene mutations in lung cancer cell lines. Statistical significance of $^{*}p<0.05$ and $^{**}p<0.01$, respectively.

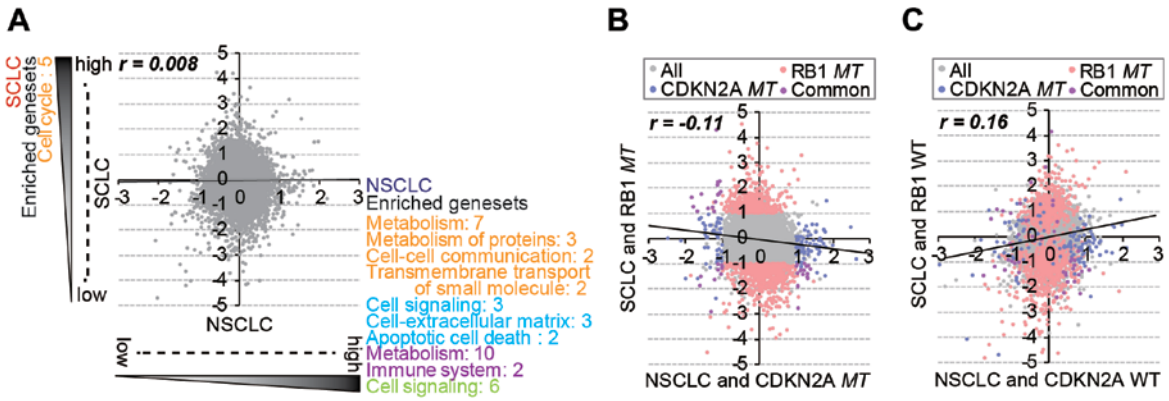

Figure 2. Comparison of gene expression in SCLC and NSCLC with the mutational status of *RB1* and *CDKN2A*. (A) The expression change of a total of 22,357 gene probes in SCLC and NSCLC cell lines. Major categories of the gene sets significantly ($p<0.01$) over-enriched for each gene expression were analyzed using gene set enrichment analysis (GSEA). Gene sets from different pathway DBs (orange, Reactome; sky-blue, PID; purple, KEGG; and green, Biocarta) were collected. The number indicates the number of gene sets per category. (B) Comparison of gene expressional change in *RB1*-mutated SCLC and *CDKN2A*-mutated NSCLC. Red represents 1,208 *RB1*-mutated SCLC-specific gene signatures and blue represents 159 *RB1*-mutated SCLC-specific gene signatures (>2-fold change and $p<0.01$). A total of 42 gene probes were commonly selected between them. (C) Comparison of gene expression change in SCLC and NSCLC cell lines with *RB1* and *CDKN2A* wild-type, respectively. The colored gene signatures were consistent with (B). The expressional change for each gene probe was calculated by the $\log_2$ fold change via the median across 318 cell lines. The *r* value represents the Pearson correlation coefficient.

have been observed in the lung cancer subtypes SCLC and NSCLC (4,13). Based on the analysis of mutation frequencies across 318 cell lines, we found the general exclusiveness of *RB1* and *CDKN2A* mutations in diverse cancer lineages (Fig. 1A). *RB1* mutations were significantly enriched in urinary tract and lung cancer cell lines yet rarely found in liver, renal, pancreatic and skin cancers, in which *CDKN2A* mutations were frequent. Furthermore, among 71 lung cancer cell lines, 25 SCLC-derived cells were significantly enriched with *RB1* mutations, whereas 46 NSCLCs predominantly contained *STK11, KRAS* and *CDKN2A* mutations (Fig. 1B). Taken together, the mutations of *RB1* and *CDKN2A* genes, which belong to a common functional pathway, were clearly exclusive from each other among frequently mutated genes in diverse cancer cell lines (Fig. 1C).

Differential gene expression profiles between RB1mt SCLCs and CDKN2Amt NSCLCs. To find lineage-independent, mutation-specific gene expression patterns, we classified 9, 16, 22 and 24 cell line samples into four groups, RB1*wt* SCLC, RB1*mt* SCLC, CDKN2A*wt* NSCLC and CDKN2A*mt* NSCLC, and analyzed the group-specific gene expression patterns using DNA microarray data. There was no general correlation of gene expression between the SCLC and NSCLC cell lines (Fig. 2A), and significantly enriched gene sets were also different between the lung subtypes. However, RB1*mt* SCLC

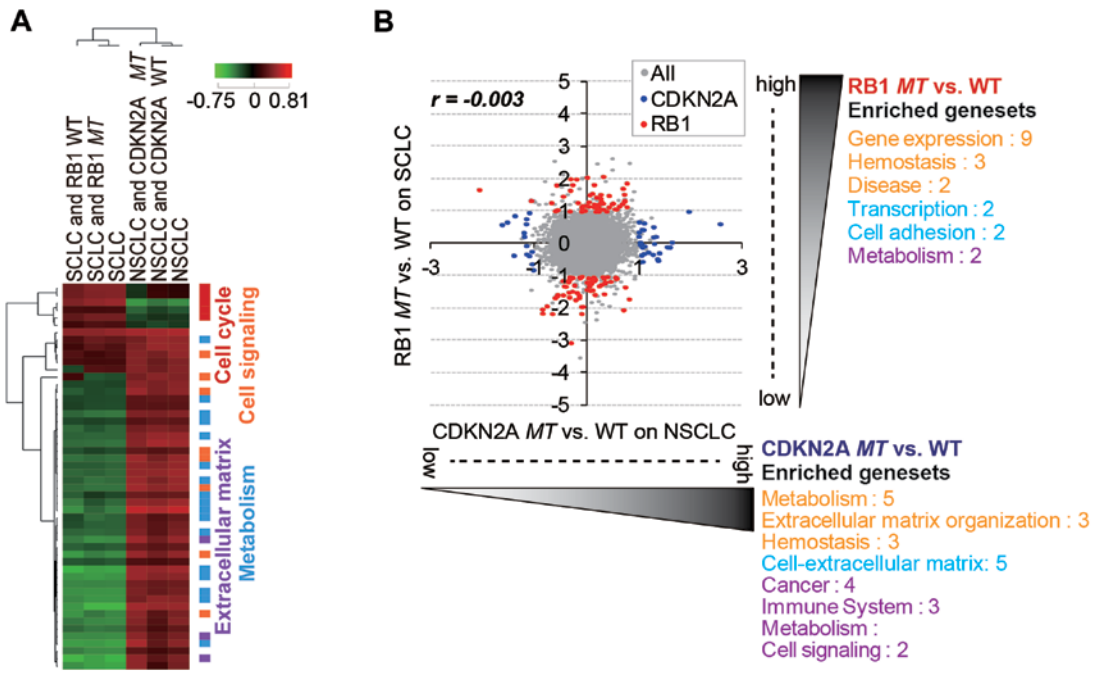

Figure 3. RB1*mt*- and CDKN2A*mt*-specific gene signatures in SCLC and NSCLC cells. (A) Enrichment score (ES) map of significantly ($p<0.01$) over-enriched gene sets in SCLC and NSCLC cell lines. Each subtype was further divided by *RB1* or *CDKN2A* mutational status. The color index on the right side represents the functional category of clustered gene sets. The individual gene expression level in Fig. 2 was used for gene set enrichment analysis (GSEA). (B) Comparison of gene expression change along *RB1* and *CDKN2A* mutations. The red color represents 159 transcription markers specific to the *RB1* mutation, and blue represents 122 transcription markers specific to the *CDKN2A* mutation (>2-fold change and $p<0.05$). The complete list of the selected markers is available in Table I and II. The scale of the plot is $\log_2$ fold change of differential gene expression. It was calculated by the differences of average $\log_2$ gene expression between mutation and wild-type cell lines in a given subtype. Major categories of the gene sets significantly ($p<0.01$) over-enriched for each gene expression were analyzed by GSEA. Gene sets from different pathway DBs (orange, Reactome; sky-blue, PID; purple, KEGG; and green, Biocarta) were collected. The value next to each category indicates the number of sub-gene sets. The *r* value represents the Pearson correlation coefficient.

and CDKN2A*mt* NSCLC cells showed a negative correlation in gene expression (Fig. 2B), whereas RB1*wt* SCLC and CDKN2A*wt* NSCLC exhibited a positive correlation (Fig. 2C). This observation indicated that *RB1* and *CDKN2A* mutations caused lineage-specific distinctive changes in gene expression.

Our analysis showed that the lineage difference was generally more important than *RB1* and *CDKN2A* mutational status in the differential gene expression pattern (Fig. 3A). Thus, we attempted to identify RB1*mt*- and CDKN2A*mt*-specific gene signatures by separately analyzing SCLC and NSCLC cells (Fig. 3B). As a result, we were able to identify distinct mutation-specific gene signatures for which expression was significantly regulated (>2-fold change and $p<0.05$) in each subtype (Tables I and II). Of note, the significantly over-enriched ($p<0.01$) gene sets (functional categories of selected gene signatures) generally did not overlap between the two mutation groups (Fig. 3B). The upregulated gene sets with *RB1* mutation in SCLC cell lines mainly belonged to functional categories of transcription. The hit list included known target genes of E2F, which are released and activated upon *RB1* inactivation (28). The upregulated genes upon *CDKN2A* mutation in NSCLC cell lines were largely enriched in the gene sets of extracellular matrix and metabolism. Genes related to the extracellular matrix are known to be important factors for enhancing tumorigenicity and promoting metastasis (29). Although CDKN2A and RB1 are known to function in the same pathway of cell cycle regulation, inactivation of the mutations might have a different functional role in cancer development or progression in SCLC and NSCLC subtypes.

Specific change in total proteins and phosphoproteins in RB1 and CDKN2A mutations. We characterized the differential regulation of *RB1* and *CDKN2A* mutations at the protein level using RPPA data of 77 pan- and 38 phospho-antibodies for 89 proteins across 179 cancer cell lines. Consistent with the patterns of gene expression data, the overall protein expression and phosphorylation status were inversely correlated between RB1*mt* SCLC and CDKN2A*mt* NSCLC cell lines (Fig. 4). Thus, the mutational effect of *RB1* and *CDKN2A* genes were separately analyzed in SCLC and NSCLC cell lines (Fig. 5). The results showed that β-catenin was commonly overexpressed in both *RB1* and *CDKN2A* mutants. Wnt/β-catenin overexpression has been extensively reported in lung cancer (30), and the overexpression of β-catenin might be maintained by the mutational effect of both *RB1* and *CDKN2A* genes. The *RB1* mutation specifically regulated PTEN, STAT, mTOR, p53 expression and MAPK phosphorylation in SCLC cells. However, the *CDKN2A* mutation altered the expression of JNK2 and cKIT and the phosphorylation status of AKT, STAT3 and AMPKa.

MAPK (T202), which is significantly ($p<0.05$) phosphorylated in *RB1*-mutated SCLC cancer cell lines, has an important role in transcriptional regulation of targeting transcription factors such as c-Jun, c-Fos, and c-Myc (31). This observation is consistent with the DNA microarray data (Fig. 3B) for RB1*mt* SCLC cells, which are enriched in the functional categories of transcription. AKT is specifically phosphorylated (S473, T308) in CDKN2A*mt* NSCLC and related to focal adhesion (32), which is the enriched gene set of CDKN2A*mt* NSCLC from

Table I. The RB1*mt*-specific gene signatures in SCLC.

Upregulated genes specific to RB1*mt*				Downregulated genes specific to RB1*mt*			
ProbeID	Symbol	log_2 fold change	p-value	ProbeID	Symbol	log_2 fold change	p-value
231736_x_at	MGST1	2.083	0.001	202834_at	AGT	-3.059	0
218847_at	IGF2BP2	2.058	0.011	1566764_at	MACC1	-2.16	0.035
202620_s_at	PLOD2	2.01	0.002	205501_at	PDE10A	-2.159	0.004
213139_at	SNAI2	2.002	0.016	204044_at	QPRT	-2.149	0.004
206332_s_at	IFI16	1.879	0.03	239503_at	Unknown	-2.041	0
235763_at	SLC44A5	1.829	0.009	208891_at	DUSP6	-2.019	0.006
204646_at	DPYD	1.828	0.005	1560652_at	Unknown	-1.943	0.019
202016_at	MEST	1.817	0.003	203881_s_at	DMD	-1.937	0.006
226225_at	MCC	1.717	0.045	208892_s_at	DUSP6	-1.921	0.005
217028_at	CXCR4	1.675	0.023	206218_at	MAGEB2	-1.732	0.013
214597_at	SSTR2	1.655	0.038	203132_at	RB1	-1.709	0.006
210839_s_at	ENPP2	1.557	0.04	205305_at	FGL1	-1.67	0.006
203038_at	PTPRK	1.531	0.001	201328_at	ETS2	-1.663	0.005
222553_x_at	OXR1	1.528	0.003	205110_s_at	FGF13	-1.651	0.036
1558217_at	SLFN13	1.515	0.045	209365_s_at	ECM1	-1.61	0.014
1565162_s_at	MGST1	1.493	0.016	210102_at	VWA5A	-1.597	0.005
204620_s_at	VCAN	1.47	0.011	209468_at	LRP5	-1.583	0.001
221731_x_at	VCAN	1.44	0.018	1558882_at	LOC401233	-1.574	0.032
218197_s_at	OXR1	1.409	0.006	219750_at	TMEM144	-1.572	0.034
205229_s_at	COCH	1.338	0.006	223748_at	SLC4A11	-1.552	0.002
203184_at	FBN2	1.338	0.026	205601_s_at	HOXB5	-1.511	0.023
205027_s_at	MAP3K8	1.311	0.004	209803_s_at	PHLDA2	-1.495	0.038
204030_s_at	SCHIP1	1.308	0.038	212268_at	SERPINB1	-1.467	0.001
241400_at	Unknown	1.296	0.006	1569191_at	ZNF826	-1.448	0.022
1555788_a_at	TRIB3	1.274	0.034	212188_at	KCTD12	-1.43	0.002
211675_s_at	MDFIC	1.272	0.012	241672_at	C13orf36	-1.414	0.033
229465_s_at	PTPRS	1.255	0.008	219305_x_at	FBXO2	-1.337	0.015
225093_at	UTRN	1.255	0.042	1554472_a_at	PHF20L1	-1.317	0
205122_at	TMEFF1	1.251	0.01	203028_s_at	CYBA	-1.308	0.047
219489_s_at	NXN	1.238	0.035	228726_at	Unknown	-1.303	0.01
225056_at	SIPA1L2	1.237	0.011	204158_s_at	TCIRG1	-1.302	0.006
208949_s_at	LGALS3	1.235	0.021	211538_s_at	HSPA2	-1.279	0.035
201063_at	RCN1	1.229	0.033	220082_at	PPP1R14D	-1.259	0.008
235244_at	CCDC58	1.184	0.032	203005_at	LTBR	-1.257	0.011
210978_s_at	TAGLN2	1.184	0.005	229964_at	C9orf152	-1.23	0.036
233903_s_at	SGEF	1.182	0.003	203961_at	NEBL	-1.212	0.032
205123_s_at	TMEFF1	1.177	0.019	224577_at	ERGIC1	-1.206	0.002
200897_s_at	PALLD	1.164	0.018	238021_s_at	CRNDE	-1.189	0.022
200916_at	TAGLN2	1.161	0.015	223041_at	CD99L2	-1.182	0.001
215127_s_at	RBMS1	1.143	0.03	205586_x_at	VGF	-1.182	0.008
202887_s_at	DDIT4	1.141	0.005	239278_at	Unknown	-1.163	0.013
212636_at	QKI	1.137	0.014	213689_x_at	FAM69A	-1.157	0.005
214877_at	CDKAL1	1.134	0.03	232099_at	PCDHB16	-1.153	0.028
227197_at	SGEF	1.129	0.005	219256_s_at	SH3TC1	-1.153	0.005
224918_x_at	MGST1	1.12	0.02	227943_at	Unknown	-1.141	0.004
227522_at	CMBL	1.08	0.007	210538_s_at	BIRC3	-1.138	0.024

Table I. Continued.

Upregulated genes specific to RB1*mt*				Downregulated genes specific to RB1*mt*			
ProbeID	Symbol	log_2 fold change	p-value	ProbeID	Symbol	log_2 fold change	p-value
206385_s_at	ANK3	1.073	0.042	1568838_at	LOC100132169	-1.117	0.032
226464_at	C3orf58	1.072	0.01	229872_s_at	LOC100132999	-1.099	0.021
1568720_at	ZNF506	1.054	0.04	1555579_s_at	PTPRM	-1.09	0.043
201656_at	ITGA6	1.04	0.028	224997_x_at	H19	-1.082	0.032
212190_at	SERPINE2	1.034	0.037	213005_s_at	KANK1	-1.081	0.01
204995_at	CDK5R1	1.022	0.017	219371_s_at	KLF2	-1.076	0.013
210512_s_at	VEGFA	1.02	0.037	37408_at	MRC2	-1.074	0.01
226419_s_at	FLJ44342	1.015	0.001	224391_s_at	SIAE	-1.059	0.01
210735_s_at	CA12	1.011	0.032	201329_s_at	ETS2	-1.053	0.022
65588_at	LOC388796	1.002	0.009	205016_at	TGFA	-1.049	0.007
213857_s_at	CD47	1.001	0.002	227384_s_at	LOC727820	-1.043	0.002
208622_s_at	EZR	1.001	0.001	228010_at	PPP2R2C	-1.033	0.031
				209500_x_at	TNFSF12/ TNFSF13	-1.031	0.019
				224576_at	ERGIC1	-1.031	0.007
				236719_at	Unknown	-1.025	0.004
				227001_at	NIPAL2	-1.021	0.006
				230722_at	BNC2	-1.019	0.047
				204682_at	LTBP2	-1.007	0.024

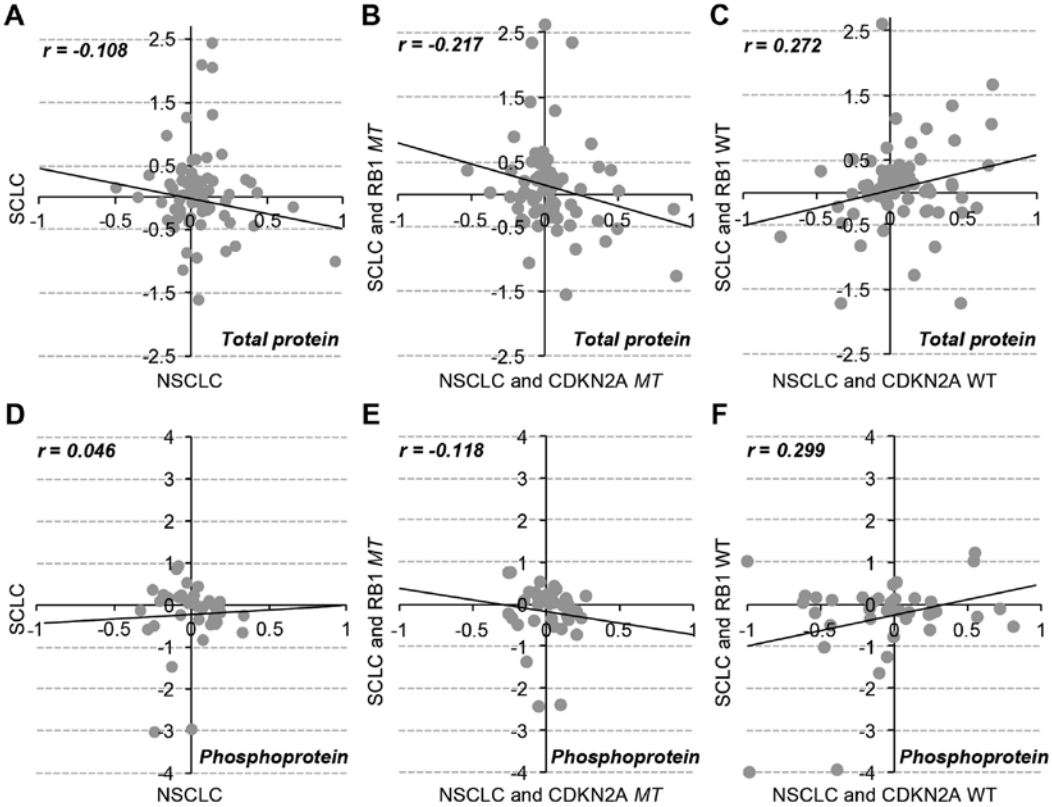

Figure 4. Comparison of protein expression and phosphorylation in SCLC and NSCLC with the mutational status of *RB1* and *CDKN2A*. Protein expression change of a total of 77 pan-antibodies was compared between (A) SCLC and NSCLC, (B) *RB1*-mutated SCLC and *CDKN2A*-mutated NSCLC, and (C) SCLC and NSCLC with *RB1* and *CDKN2A* wild-type cell lines, respectively. Protein phosphorylation change of a total of 38 phospho-antibodies was compared between (D) SCLC and NSCLC, (E) *RB1*-mutated SCLC and *CDKN2A*-mutated NSCLC, and (F) SCLC and NSCLC with *RB1* and *CDKN2A* wild-type cell lines, respectively. The phosphorylation change for each protein phospho-antibody was calculated by the log_2 fold change via the median across 179 cell lines. The *r* value represents the Pearson correlation coefficient.

Table II. The CDKN2A*mt*-specific gene signatures in NSCLC.

Upregulated genes specific to CDKN2A*mt*				Downregulated genes specific to CDKN2A*mt*			
ProbeID	Symbol	log_2 fold change	p-value	ProbeID	Symbol	log_2 fold change	p-value
236694_at	CYorf15A	2.585	0.001	228956_at	UGT8	-1.618	0.001
211980_at	COL4A1	1.978	0.006	209644_x_at	CDKN2A	-1.52	0.004
213725_x_at	XYLT1	1.654	0.023	225681_at	CTHRC1	-1.396	0.014
204971_at	CSTA	1.615	0.022	1554242_a_at	COCH	-1.373	0.008
209970_x_at	CASP1	1.566	0.001	218820_at	C14orf132	-1.199	0.012
225688_s_at	PHLDB2	1.412	0.017	200884_at	CKB	-1.191	0.001
202638_s_at	ICAM1	1.388	0.011	227623_at	Unknown	-1.156	0.018
222453_at	CYBRD1	1.377	0.016	207558_s_at	PITX2	-1.151	0.014
1562102_at	AKR1C1	1.344	0.048	236302_at	PPM1E	-1.151	0.009
208782_at	FSTL1	1.312	0.014	209198_s_at	SYT11	-1.145	0.007
211340_s_at	MCAM	1.299	0.002	1560023_x_at	Unknown	-1.097	0.01
210004_at	OLR1	1.299	0.01	214321_at	NOV	-1.094	0.035
202008_s_at	NID1	1.286	0.004	205229_s_at	COCH	-1.061	0.031
202350_s_at	MATN2	1.197	0.012	223551_at	PKIB	-1.045	0.046
239999_at	Unknown	1.126	0.033	230130_at	Unknown	-1.04	0.049
205407_at	RECK	1.117	0.014	212706_at	LOC100286937/ LOC100287164/ RASA4	-1.019	0.003
203304_at	BAMBI	1.113	0.012				
228698_at	SOX7	1.104	0.014				
227051_at	Unknown	1.088	0.036				
201939_at	PLK2	1.082	0.017				
209087_x_at	MCAM	1.081	0.007				
206165_s_at	CLCA2	1.067	0.025				
227178_at	CUGBP2	1.067	0.012				
227253_at	CP	1.044	0.015				
212262_at	QKI	1.043	0.002				
202998_s_at	LOXL2	1.039	0.006				
214022_s_at	IFITM1	1.021	0.034				
211366_x_at	CASP1	1.019	0.001				
222446_s_at	BACE2	1.014	0.009				

DNA microarray analysis. Furthermore, PTEN, which was overexpressed in RB1*mt* SCLC cells (Fig. 5A), is a well-known negative regulator of AKT activation (33), suggesting that AKT-mediated signaling might be exclusively activated by CDKN2A*mt* in NSCLC, not by RB1*mt* in SCLC. Both proteome and transcriptome data analyses demonstrated that exclusive *RB1* and *CDKN2A* mutations in different subtypes of lung cancer included a differential change of gene expression and protein regulation, even though *RB1* and *CDKN2A* are in the same cell cycle-related pathway.

Synthetic lethality of reciprocal regulation of RB1 and CDKN2A expression. Through the systematic analysis of transcriptome and proteome data, we found unique mRNA and protein regulation patterns induced by the mutation of either the *RB1* gene or the *CDKN2A* gene (Fig. 6A). Furthermore, we investigated the synergistic negative effect on cancer growth by simultaneous functional loss (or knockdown) of these two genes. We performed a viability assay with diverse lung cancer cell lines with the combined knockdown of *RB1* and *CDKN2A* genes using siRNA-mediated gene depletion. As a result, the knockdown of one of these genes decreased the viability of cells harboring a mutation of the other gene (Fig. 6B). The viability of *CDKN2A*-mutant cell lines was significantly decreased by knockdown of *RB1*; similarly, *RB1*-mutant cell lines were inhibited by *CDKN2A* depletion. Consistently, the simultaneous depletion of *RB1* and *CDKN2A* genes significantly decreased the viability of lung cell lines harboring wild-types of these genes (Fig. 6C). However, the single knockdown of either the *RB1* gene or the *CDKN2A* gene did not effectively reduce viability in these wild-type cell lines. In conclusion, the functional inhibition of the *RB1* or *CDKN2A* gene in CDKN2A*mt* or RB1*mt* cancer cells, respectively, might be a promising therapeutic approach in SCLC or NSCLC lung cancers. The present

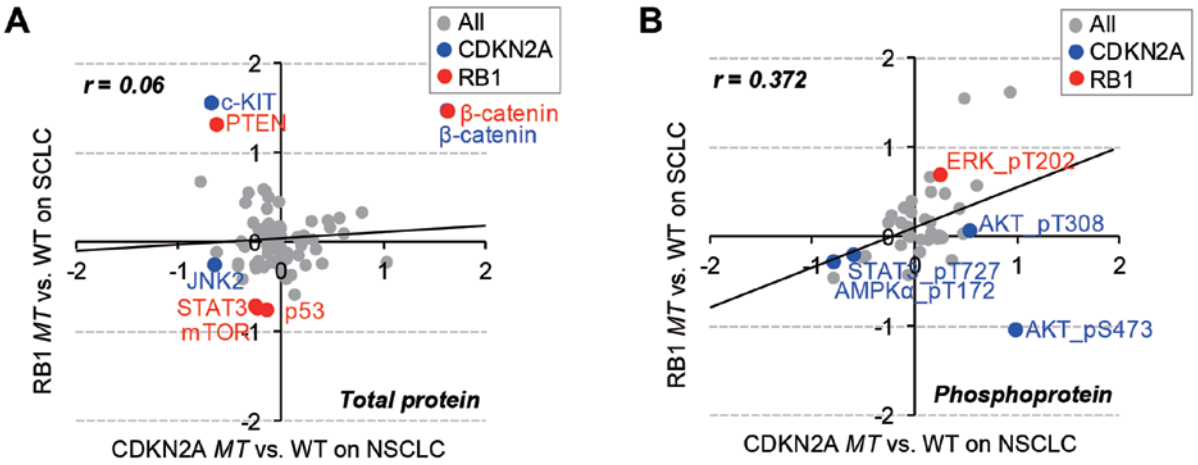

Figure 5. Protein and phosphoprotein signatures specific to *RB1* or *CDKN2A* mutations. (A) Comparison of differential protein expression (77 pan-antibody data) between *RB1* and *CDKN2A* mutations. (B) Comparison of differential protein phosphorylation (38 phospho-antibody data) between *RB1* and *CDKN2A* mutations. The red color represents protein markers specific to the *RB1* mutation, and blue represents protein markers specific to the *CDKN2A* mutation (>1-fold change and $p<0.05$). The scale of the plots is the $\log_2$ fold change of protein expression and phosphorylation, respectively. The value was calculated by the differences of average $\log_2$ expression or phosphorylation level between mutation and wild-type cell lines in the given subtype. The *r* value represents the Pearson correlation coefficient.

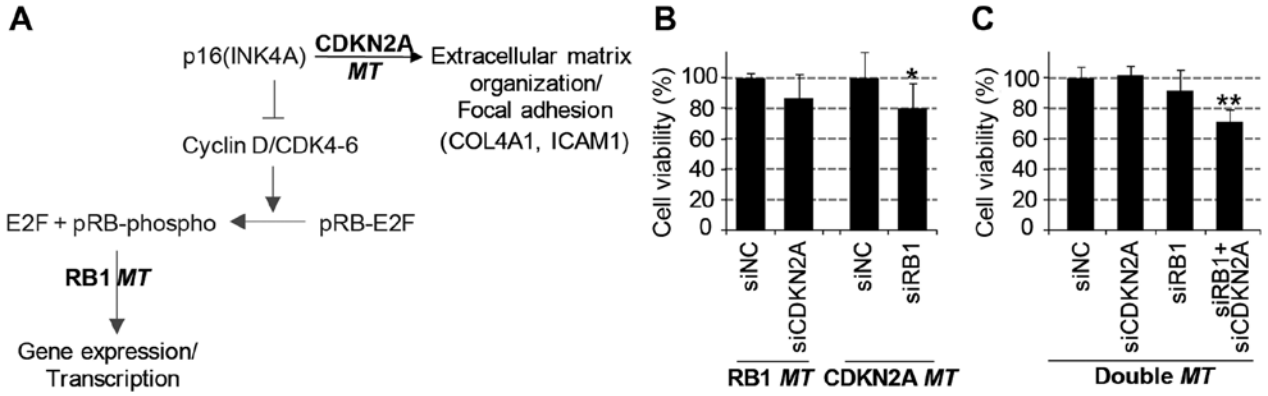

Figure 6. Differential viability change of lung cancer subtypes induced by reciprocal knockdown of the *RB1* and/or *CDKN2A* genes. (A) A schematic summary of biological functions dysregulated by the mutation status of *RB1* and *CDKN2A*. (B) The effects of siRB1 and siCDKN2A in lung cell lines with *CDKN2A* mutations (NCI-H82 and NCI-H524) and *RB1* mutations (NCI-H460, A549, NCI-H322M, and NCI-H226), respectively. (C) The effect of single- or double-knockdown of *RB1* and *CDKN2A* gene expression on the viability of *RB1*- and *CDKN2A*-positive cell lines (EKVX, NCI-H23, NCI-H1395, and NCI-H1993). The cells were incubated in siRB1 and siCDKN2A and cultured for 72 h. Cell viability was determined using a CellTiter-Blue assay. The siRNA-mediated gene depletion efficacy of *RB1* or *CDKN2A* in each tested cell line was evaluated (data not shown). The % cell viability was calculated using siNC as the negative control for each siRNA treatment. $^{*}p<0.05$ and $^{**}p<0.01$ between the compared groups.

study on differential proteome and transcriptome profiles between two mutant groups provides mechanistic insights into the synthetic lethality of RB1 and CDKN2A mutations.

Acknowledgements

This study was supported by Sookmyung Women's University Research Grant 1-1303-0160.

References

1. Kim N, He N, Kim C, Zhang F, Lu Y, Yu Q, Stemke-Hale K, Greshock J, Wooster R, Yoon S, *et al*: Systematic analysis of genotype-specific drug responses in cancer. Int J Cancer 131: 2456-2464, 2012.
2. Settleman J: Cell culture modeling of genotype-directed sensitivity to selective kinase inhibitors: Targeting the anaplastic lymphoma kinase (ALK). Semin Oncol 36 (Suppl 1): S36-S41, 2009.
3. He N, Kim N, Song M, Park C, Kim S, Park EY, Yim HY, Kim K, Park JH, Kim KI, *et al*: Integrated analysis of transcriptomes of cancer cell lines and patient samples reveals STK11/LKB1-driven regulation of cAMP phosphodiesterase-4D. Mol Cancer Ther 13: 2463-2473, 2014.
4. Knudsen ES and Knudsen KE: Tailoring to RB: Tumour suppressor status and therapeutic response. Nat Rev Cancer 8: 714-724, 2008.
5. Xie Z and Liu D: Pathogenesis of molecular signaling pathways changes in smoking-induced lung cancer. Zhongguo Fei Ai Za Zhi 12: 1202-1205, 2009 (in Chinese).
6. Serrano M, Hannon GJ and Beach D: A new regulatory motif in cell-cycle control causing specific inhibition of cyclin D/CDK4. Nature 366: 704-707, 1993.
7. Hernando E, Nahlé Z, Juan G, Diaz-Rodriguez E, Alaminos M, Hemann M, Michel L, Mittal V, Gerald W, Benezra R, *et al*: Rb inactivation promotes genomic instability by uncoupling cell cycle progression from mitotic control. Nature 430: 797-802, 2004.
8. Dyson N: The regulation of E2F by pRB-family proteins. Genes Dev 12: 2245-2262, 1998.
9. Classon M and Harlow E: The retinoblastoma tumour suppressor in development and cancer. Nat Rev Cancer 2: 910-917, 2002.

10. Kosaka T, Yatabe Y, Endoh H, Kuwano H, Takahashi T and Mitsudomi T: Mutations of the epidermal growth factor receptor gene in lung cancer: Biological and clinical implications. Cancer Res 64: 8919-8923, 2004.
11. Shigematsu H, Lin L, Takahashi T, Nomura M, Suzuki M, Wistuba II, Fong KM, Lee H, Toyooka S, Shimizu N, *et al*: Clinical and biological features associated with epidermal growth factor receptor gene mutations in lung cancers. J Natl Cancer Inst 97: 339-346, 2005.
12. Singh B, Reddy PG, Goberdhan A, Walsh C, Dao S, Ngai I, Chou TC, O-Charoenrat P, Levine AJ, Rao PH, *et al*: p53 regulates cell survival by inhibiting PIK3CA in squamous cell carcinomas. Genes Dev 16: 984-993, 2002.
13. Blanco R, Iwakawa R, Tang M, Kohno T, Angulo B, Pio R, Montuenga LM, Minna JD, Yokota J and Sanchez-Cespedes M: A gene-alteration profile of human lung cancer cell lines. Hum Mutat 30: 1199-1206, 2009.
14. Etemadmoghadam D, Weir BA, Au-Yeung G, Alsop K, Mitchell G, George J, Davis S, D'Andrea AD, Simpson K, Hahn WC, *et al*; Australian Ovarian Cancer Study Group: Synthetic lethality between CCNE1 amplification and loss of BRCA1. Proc Natl Acad Sci USA 110: 19489-19494, 2013.
15. Shoemaker RH, Monks A, Alley MC, Scudiero DA, Fine DL, McLemore TL, Abbott BJ, Paull KD, Mayo JG and Boyd MR: Development of human tumor cell line panels for use in disease-oriented drug screening. Prog Clin Biol Res 276: 265-286, 1988.
16. Greshock J, Bachman KE, Degenhardt YY, Jing J, Wen YH, Eastman S, McNeil E, Moy C, Wegrzyn R, Auger K, *et al*: Molecular target class is predictive of in vitro response profile. Cancer Res 70: 3677-3686, 2010.
17. Forbes SA, Bindal N, Bamford S, Cole C, Kok CY, Beare D, Jia M, Shepherd R, Leung K, Menzies A, *et al*: COSMIC: mining complete cancer genomes in the Catalogue of Somatic Mutations in Cancer. Nucleic Acids Res 39 (Database): D945-D950, 2011.
18. Kim N, He N and Yoon S: Cell line modeling for systems medicine in cancers (Review). Int J Oncol 44: 371-376, 2014.
19. Jeong E, He N, Park H, Song M, Kim N, Lee S and Yoon S: MACE: mutation-oriented profiling of chemical response and gene expression in cancers. Bioinformatics 31: 1508-1514, 2015.
20. McDermott U, Sharma SV, Dowell L, Greninger P, Montagut C, Lamb J, Archibald H, Raudales R, Tam A, Lee D, *et al*: Identification of genotype-correlated sensitivity to selective kinase inhibitors by using high-throughput tumor cell line profiling. Proc Natl Acad Sci USA 104: 19936-19941, 2007.
21. Vasudevan KM, Barbie DA, Davies MA, Rabinovsky R, McNear CJ, Kim JJ, Hennessy BT, Tseng H, Pochanard P, Kim SY, *et al*: AKT-independent signaling downstream of oncogenic PIK3CA mutations in human cancer. Cancer Cell 16: 21-32, 2009.
22. Craft CS, Zou W, Watkins M, Grimston S, Brodt MD, Broekelmann TJ, Weinbaum JS, Teitelbaum SL, Pierce RA, Civitelli R, *et al*: Microfibril-associated glycoprotein-1, an extracellular matrix regulator of bone remodeling. J Biol Chem 285: 23858-23867, 2010.
23. Stemke-Hale K, Gonzalez-Angulo AM, Lluch A, Neve RM, Kuo WL, Davies M, Carey M, Hu Z, Guan Y, Sahin A, *et al*: An integrative genomic and proteomic analysis of PIK3CA, PTEN, and AKT mutations in breast cancer. Cancer Res 68: 6084-6091, 2008.
24. Tibes R, Qiu Y, Lu Y, Hennessy B, Andreeff M, Mills GB and Kornblau SM: Reverse phase protein array: validation of a novel proteomic technology and utility for analysis of primary leukemia specimens and hematopoietic stem cells. Mol Cancer Ther 5: 2512-2521, 2006.
25. Agresti A and John Wiley & Sons: Categorical Data Analysis. Wiley Series in Probability and Statistics Wiley-Interscience, New York, 2002.
26. Kim N, Park H, He N, Lee HY and Yoon S: QCanvas: An Advanced Tool for Data Clustering and Visualization of Genomics Data. Genomics Inform 10: 263-265, 2012.
27. Subramanian A, Tamayo P, Mootha VK, Mukherjee S, Ebert BL, Gillette MA, Paulovich A, Pomeroy SL, Golub TR, Lander ES, *et al*: Gene set enrichment analysis: a knowledge-based approach for interpreting genome-wide expression profiles. Proc Natl Acad Sci USA 102: 15545-15550, 2005.
28. Rocco JW and Sidransky D: p16(MTS-1/CDKN2/INK4a) in cancer progression. Exp Cell Res 264: 42-55, 2001.
29. Gilkes DM, Semenza GL and Wirtz D: Hypoxia and the extracellular matrix: drivers of tumour metastasis. Nat Rev Cancer 14: 430-439, 2014.
30. Mazieres J, He B, You L, Xu Z and Jablons DM: Wnt signaling in lung cancer. Cancer Lett 222: 1-10, 2005.
31. Chang F, Steelman LS, Lee JT, Shelton JG, Navolanic PM, Blalock WL, Franklin RA and McCubrey JA: Signal transduction mediated by the Ras/Raf/MEK/ERK pathway from cytokine receptors to transcription factors: potential targeting for therapeutic intervention. Leukemia 17: 1263-1293, 2003.
32. Wang S and Basson MD: Akt directly regulates focal adhesion kinase through association and serine phosphorylation: Implication for pressure-induced colon cancer metastasis. Am J Physiol Cell Physiol 300: C657-C670, 2011.
33. Song MS, Salmena L and Pandolfi PP: The functions and regulation of the PTEN tumour suppressor. Nat Rev Mol Cell Biol 13: 283-296, 2012.